Proceedings of the Sixth International Conference on
Railway Technology: Research, Development and Maintenance
Edited by: J. Pombo
Civil-Comp Conferences, Volume 7, Paper 16.4
Civil-Comp Press, Edinburgh, United Kingdom, 2024
ISSN: 2753-3239, doi: 10.4203/ccc.7.16.4

Model Predictive Control of a Disturbed Maglev System

M. Liu,[1,2] S. Fu,[3,4] H. Wu,[1,2] X. Liang[3,4] and X. Zeng[1,2]

[1]Key Laboratory for Mechanics in Fluid Solid Coupling Systems
Institute of Mechanics, Chinese Academy of Sciences, Beijing, China
[2]School of Engineering Science
University of Chinese Academy of Sciences, Beijing, China
[3]Qingdao Sifang Co., Ltd., CRRC, China
[4]State Key Laboratory, High-speed Maglev Transportation Technology,Qingdao, China

Abstract

To improve the suspension control effect of the high-speed maglev train, a model predictive control (MPC) algorithm considering the disturbance force is designed based on the electromagnet suspension system unit of the maglev train. When constructing MPC algorithms, the influence of disturbance force on the system is commonly disregarded. However, neglecting this effect may lead to the failure of the predictive model and subsequently impact the performance of the control algorithm. In the paper, the disturbance force is incorporated as input to establish the state prediction model of the suspension system. The predicted values are then corrected by the error between the actual and the predicted state. Subsequently, the objective function and relevant constraints for the suspension system are designed, and the optimal control quantity of the system is obtained by rolling optimization. Finally, the performance of the MPC controller is evaluated through numerical calculations. Research results indicate that, in comparison with the traditional proportional-integral-derivative (PID) feedback controller, the MPC controller proposed effectively suppresses the fluctuation of the suspension gap. Moreover, incorporating the disturbance force into the predictive model of the system's state can further optimize the performance of the MPC controller.

Keywords: model predictive control, high-speed maglev train, suspension fluctuation, state prediction, rolling optimization, suspension control

1 Introduction

Electromagnetic suspension (EMS) trains rely on the electromagnetic force between the suspension electromagnet and the track to counteract gravity, achieving suspension [1]. This approach avoids contact between the track and the vehicle. Compared with traditional vehicles, EMS maglev trains have the advantages of low energy consumption, low environmental impact, low noise, less maintenance, and strong climbing ability [2-3]. The suspension system of the EMS maglev train is inherently unstable and depends on real-time control. Therefore, to achieve the reliable and stable performance of the train, we must focus on the enhancement of the suspension control system.

Currently, the EMS maglev train adopts the proportional-integral-derivative (PID) control algorithm [1, 4]. The PID algorithm constitutes a control according to the deviation between the train's desired and actual suspension gap. This deviation is linearly combined by proportional, integral, and differential to compute a control quantity, ensuring the stable suspension of the train. However, this PID algorithm has some disadvantages, including the control parameters are difficult to change after loading and susceptibility to the impact of model errors during the design phase. These factors lead to the poor robustness and stability of the off-line PID control. With the continuous improvement of the speed of maglev trains, the influence of aerodynamic load becomes more and more significant. To control the suspension system more effectively, many more advanced control algorithms are applied to the suspension control system of the maglev train, such as sliding mode control [5-6], robust control [7], fuzzy control [8-9], and so on. For example, Nath [10] introduces fuzzy logic into the suspension system of the simplified maglev train and combines it with the traditional control algorithm to design a fuzzy controller. The calculation results show that this controller exhibits good performance in efficiency and self-regulation compared to a simple PID controller. However, fuzzy control relies heavily on expert experience. Yang and colleagues [11] propose a dynamic sliding surface based on the disturbance estimation of the suspension system. Following this, they establish a continuous dynamic sliding mode control (CDSMC) method that applies to the suspension control system. Results show that this method can improve the performance and stability of the suspension system. Gao [12] proposes a control method based on sliding mode periodic adaptive learning control (SM-PALC). This approach aims to reduce the position error of the maglev train suspension system and improve the robustness of the control system. However, this algorithm depends on the accuracy of the model. Ni [13] presents an improved nonlinear mathematical model of electromagnetic force for the suspension system of the EMS maglev train. This model is utilized to develop a robust controller. Simulation and semi-physical experiments verify that the controller can make the system track the target trajectory stably under disturbance. Benomair [14] proposes a fuzzy sliding mode controller with a nonlinear observer for the magnetic suspension system. The simulation results demonstrate that this controller facilitates better stable suspension of the system.

Nevertheless, all the aforementioned algorithms control after the changes in the vehicle state, and they are not out of the scope of traditional feedback control. Due to the existence of time delay, the suspension system state may have changed greatly when the time feedback control is executed, which affects the stability of the system. At high speeds, the conventional feedback control algorithm for the maglev train is susceptible to experiencing control failures. To improve the insufficiency of offline optimization and hysteresis of traditional algorithms, this paper introduces model prediction control (MPC) into the suspension control of maglev trains. Then, an intelligent control algorithm is proposed, which can proactively control before the train state changes. This MPC algorithm utilizes the prediction model to estimate the future dynamic behavior of the system under certain control and continuously rolls forward to obtain the optimal control quantity according to the constraints [15-17]. The MPC algorithm employs a finite-time optimization strategy that rolls forward in time, which signifies that the optimization process is not a one-time offline operation but rather a repeated online procedure. In contrast, traditional control methods typically solve for a feedback control quantity offline and then continuously apply that control quantity to the system. Furthermore, the MPC algorithm can predict the future dynamic behavior of the system and control it in advance according to the difference between the actual and the expected behavior. This capability helps prevent excessive disturbance when the train encounters strong impact loads, thus it also has the advantage of feedforward control. In recent years, MPC has seen a gradual application in various control domains. Examples include trajectory tracking for autonomous vehicles [18-19], control of automobile engines [20], steering control in automobiles [21], and robot control [22]. Du [23] presents a variable predictive time-domain MPC method for improving vehicle lateral stability control of vehicles. The approach is grounded in a three-degree-of-freedom model for vehicle lateral dynamics. Simulation results demonstrate the algorithm's effectiveness in improving trajectory tracking accuracy and enhancing the lateral stability of autonomous vehicles. Chen [24] develops an optimized power management strategy for fuel cell hybrid electric vehicles using improved MPC. The reliability and effectiveness of this strategy have been verified through simulations and experiments. These research findings indicate that the MPC algorithm performs exceptionally well in controlling the target trajectory and optimizing multivariable problems within the control system. It demonstrates robustness and delivers excellent control performance.

The primary goal of controlling the suspension system of the maglev train is to maintain stable suspension close to its desired position. In addition, to meet the requirements of safety and ride comfort, the train must adhere to operational limits concerning the maximum gap and acceleration. Therefore, the control problem of maglev trains is essentially a time-varying multi-constraint optimization problem. Based on the previous research results, this paper aims to apply MPC to the suspension control system of high-speed maglev trains and propose a more efficient control algorithm. The suspension system of the maglev train consists of multiple electromagnet suspension units. Since the train adopts a modular decentralized structure, it is possible to control the train in a decentralized manner. This means that the suspension control system of the single electromagnet can be designed independently to achieve the overall design of the vehicle's suspension control system, leading to a streamlined and simplified control system design. Hence, focusing on a single electromagnet as the research subject, an MPC algorithm is developed specifically for the suspension system. Nevertheless, it is noteworthy that some scholars ignore the impact of disturbance forces during designing MPC algorithms [25]. In reality, these disturbance forces have an important influence on the dynamic response of the system. Neglecting these disturbance forces in the construction of the prediction model can result in inaccuracies in system predictions, thus affecting the controller's performance. Therefore, two prediction models are formulated—one taking into account the disturbance force and another disregarding it. Subsequently, the MPC algorithm for maglev control systems is built based on these distinct prediction models. Ultimately, the effectiveness of these algorithms is verified by numerical calculations.

2 Suspension system of single electromagnet

The vertical motion of the electromagnet for maglev trains is shown in Figure 1. Assuming that the mass of the electromagnet is *m* and the vertical downward is the positive direction, the vertical motion equation of the electromagnet can be written as:

$$m\ddot{z} = mg - F\left(i,z\right) + f_d\left(t\right) \tag{1}$$

In Equation (1), *z* represents the relative distance between the electromagnet and the track, that is, the suspension gap of the electromagnet. f_d is the disturbance force (primary suspension, lift). *F* (*i*, *z*) represents the electromagnetic force, and *i* is the control current in the electromagnet.

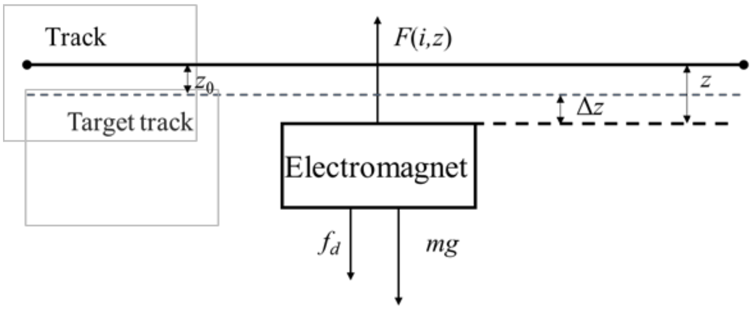

Figure 1: Electromagnet motion model.

The instantaneous inductance of the electromagnet coil is:

$$L\left(z,i\right) = \frac{\mu_0 N^2 A}{2z\left(t\right)} \tag{2}$$

In Equation (2), μ_0 represents the air permeability, *A* represents the effective area of the electromagnet, and *N* is the number of coil turns.

Assuming that the variation of the excitation current and the coil inductance is independent of each other, the electromagnetic force between the electromagnet and the track [26] can be expressed as:

$$F\left(i,z\right) = \frac{d}{dz}\{\frac{1}{2}L(z)[i(t)]^2\} = \frac{\mu_0 N^2 A[i(t)]^2}{4[z\left(t\right)]^2} \tag{3}$$

The equilibrium state of the electromagnet's stable suspension is (i_0, z_0), where i_0 represents the stable current, and z_0 denotes the stable suspension gap. Let Δi be the current disturbance relative to the equilibrium state i_0, and Δz be the gap fluctuation of the electromagnet relative to the equilibrium position z_0. The electromagnetic force in Equation (3) can be written as:

$$F=\frac{\mu_0 A N^2\left(i_0+\Delta i\right)^2}{4\left(z_0+\Delta z\right)^2} \tag{4}$$

Equation (4) is expanded by Taylor series:

$$F=\frac{\mu_0 A N^2\left(i_0+\Delta i\right)^2}{4\left(z_0+\Delta z\right)^2}=\frac{\mu_0 A N^2}{4 z_0{}^2}\left(i_0{}^2+2 i_0 \Delta i+\Delta i^2\right)\left[1-2\left(\frac{\Delta z}{z_0}\right)^1+3\left(\frac{\Delta z}{z_0}\right)^2+\cdots\right] \tag{5}$$

Ignoring the influence of higher order Δi and Δz, we obtain:

$$F(i, z)=F_0+\frac{\partial F}{\partial i} \Delta i+\frac{\partial F}{\partial z} \Delta z=\frac{\mu_0 A N^2 i_0}{4 z_0}+\frac{\mu_0 A N^2 i_0}{2 z_0{}^2} \Delta i-\frac{\mu_0 A N^2 i_0{}^2}{2 z_0{}^3} \Delta z \tag{6}$$

The linearized model of the single electromagnet's suspension system at the equilibrium point is:

$$m \Delta \ddot{z}(t)=-\Delta F+f_d=-K_i \Delta i(t)+K_z \Delta z(t)+f_d(t) \tag{7}$$

Where K_z and K_i are the gap proportionality coefficient and the current proportionality coefficient, respectively. The values of these coefficients are:

$$\begin{cases} K_Z=\dfrac{\mu_0 A N^2 i_0{}^2}{2 z_0{}^3} \\ K_i=\dfrac{\mu_0 A N^2 i_0}{2 z_0{}^2} \end{cases}$$

At the equilibrium point (z_0, i_0), there is:

$$m g=F_0\left(i_0, z_0\right)=\frac{\mu_0 N^2 A}{4}\left[\frac{i_0}{z_0}\right]^2 \tag{8}$$

Let $x_1=\Delta z,\ x_2=\Delta \dot{z},\ u=\Delta i$, $\boldsymbol{x}=\left[\begin{array}{ll}x_1 & x_2\end{array}\right]^{\mathrm{T}}$. Then the linearized state equation of the system is:

$$\begin{aligned} & \dot{\boldsymbol{x}}=\boldsymbol{A}_1 \dot{\boldsymbol{x}}+\boldsymbol{B}_1 u+\boldsymbol{G}_1 f_d \\ & y=\boldsymbol{C}_1 \boldsymbol{x} \end{aligned} \tag{9}$$

Where, $\boldsymbol{A}_1=\left[\begin{array}{cc}0 & 1 \\ \frac{K_z}{m} & 0\end{array}\right]$, $\boldsymbol{B}_1=\left[\begin{array}{c}0 \\ \frac{-K_i}{m}\end{array}\right]$, $\boldsymbol{C}_1=\left[\begin{array}{ll}1 & 0\end{array}\right]$, $\boldsymbol{G}_1=\left[\begin{array}{c}0 \\ \frac{1}{m}\end{array}\right]$

3 MPC algorithm for suspension systems

3.1 State prediction equations for electromagnets

The forward Euler method is employed to discretize the state equations in Equation (9), resulting in a linear time-invariant state space model for the electromagnet:

$$\begin{aligned} & \boldsymbol{x}(k+1)=\boldsymbol{A}_2 \boldsymbol{x}(k)+\boldsymbol{B}_2 u(k)+\boldsymbol{G}_2 f_d(k) \\ & y(k)=\boldsymbol{C}_2 \boldsymbol{x}(k) \end{aligned} \tag{10}$$

Where, $\boldsymbol{A}_2=\boldsymbol{I}+T\boldsymbol{A}_1$, $\boldsymbol{B}_2=\boldsymbol{I}+T\boldsymbol{B}_1$, $\boldsymbol{C}_2=\boldsymbol{C}_1$, $\boldsymbol{G}_2=T\boldsymbol{G}_1$. T stands for control period.

Assuming that the prediction time domain of the system is P. Recursively, the predicted value of the system state for the next n (n=1, 2, ⋯, P) moments can be obtained:

$$
\begin{aligned}
&\boldsymbol{x}(k+n)=\boldsymbol{A}_2\boldsymbol{x}(k+n-1)+\boldsymbol{B}_2u(k+n-1)+\boldsymbol{G}_2 f_d(k+n-1)\\
&=\boldsymbol{A}_2{}^P\boldsymbol{x}(k)+\boldsymbol{A}_2{}^{P-1}\boldsymbol{B}_2u(k)+\cdots+\boldsymbol{B}_2u(k+n-1)+\boldsymbol{A}_2{}^{P-1}\boldsymbol{G}_2 f_d(k)+\cdots+\boldsymbol{G}_2 f_d(k+n-1)\\
&y(k+n)=\boldsymbol{C}_2\boldsymbol{x}(k+n)
\end{aligned}
\tag{11}
$$

Combining Equation (11) into matrix form, we have:

$$
\begin{aligned}
\boldsymbol{X}_{k+1}&=\boldsymbol{A}\boldsymbol{X}_k+\boldsymbol{B}\boldsymbol{U}_k+\boldsymbol{G}\boldsymbol{F}_k\\
\boldsymbol{Y}_{k+1}&=\boldsymbol{C}\boldsymbol{X}_{k+1}
\end{aligned}
\tag{12}
$$

Where:

$$\boldsymbol{A}=\begin{pmatrix}\boldsymbol{A}_2 & \boldsymbol{A}_2{}^2 & \cdots & \boldsymbol{A}_2{}^P\end{pmatrix}^{\mathrm{T}},\boldsymbol{C}=\begin{pmatrix}\boldsymbol{C}_2 & \boldsymbol{C}_2 & \cdots & \boldsymbol{C}_2\end{pmatrix}^{\mathrm{T}}$$

$$\boldsymbol{B}=\begin{pmatrix}\boldsymbol{B}_2 & \cdots & 0 & 0\\ \boldsymbol{A}_2\boldsymbol{B}_2 & \boldsymbol{B}_2 & \cdots & 0\\ \vdots & \vdots & \ddots & \vdots\\ \boldsymbol{A}_2{}^{P-1}\boldsymbol{B}_2 & \boldsymbol{A}_2{}^{P-2}\boldsymbol{B}_2 & \cdots & \boldsymbol{B}_2\end{pmatrix}\boldsymbol{G}=\begin{pmatrix}\boldsymbol{G}_2 & \cdots & 0 & 0\\ \boldsymbol{A}_2\boldsymbol{G}_2 & \boldsymbol{G}_2 & \cdots & 0\\ \vdots & \vdots & \ddots & \vdots\\ \boldsymbol{A}_2{}^{P-1}\boldsymbol{G}_2 & \boldsymbol{A}_2{}^{P-2}\boldsymbol{G}_2 & \cdots & \boldsymbol{G}_2\end{pmatrix}$$

The disturbance at a future time is unknown, assuming that the disturbance remains constant at the current value, i.e.:

$$f_d(k+P-1)=f_d(k+1)=f_d(k) \tag{13}$$

Then the disturbance force coefficient matrix $\boldsymbol{G}$ in Equation (12) can be simplified as:

$$\boldsymbol{G}=\begin{pmatrix}\boldsymbol{G}_2\\ \boldsymbol{A}_2\boldsymbol{G}_2+\boldsymbol{G}_2\\ \vdots\\ \boldsymbol{A}_2{}^{P-1}\boldsymbol{G}_2+\cdots\boldsymbol{G}_2\end{pmatrix}$$

3.2 Feedback correction

The prediction model may exhibit errors attributed to identification inaccuracies. To address the impact of these uncertainties on the prediction model, a feedback correction is introduced in the MPC algorithm. This feedback element is designed to rectify the errors of the state prediction for the electromagnet, thereby improving the calculation accuracy of the prediction model. The specific process is as follows: At each time step, the MPC algorithm detects the actual output result and corrects the prediction result using the error between the actual and predicted state outputs of the electromagnet. This element provides predictive control feedback to momentarily correct the predicted value of the electromagnet state. The corrected prediction value of the electromagnet state at time k+n (n=1, 2, ⋯, P) is:

$$
\begin{aligned}
e_k&=y^*{}_k-y_k\\
\boldsymbol{Y}^p{}_{k+1}&=\boldsymbol{Y}_{k+1}+\delta e_k\boldsymbol{E}
\end{aligned}
\tag{14}
$$

Where $y^*{}_k$ and y_k represent the actual output and predicted output of the electromagnet state at time t_k, respectively. $\boldsymbol{Y}^p{}_{k+1}$ represents the predicted value after correction. $\boldsymbol{E}$ denotes the unit vector of dimension P*1. δ represents the feedback correction coefficient, and there is no clear and effective method to select its value. Usually, an appropriate value can be determined through empirical setups and simulation trials.

3.3 Rolling optimization

In order to guarantee a stable suspension state for the maglev vehicle during its operation, it is hoped that the state output value of the electromagnet (i.e., suspension gap) can be close to the predetermined target value. To make the electromagnet's suspension gap approach the target value in the future, the quadratic function is adopted as the performance index function of rolling optimization. We define the reference suspension gap sequence in the prediction time domain as follows:

$$\boldsymbol{R} = \begin{pmatrix} z_0(k+1) & z_0(k+2) & \cdots & z_0(k+P) \end{pmatrix}^{\mathrm{T}} \tag{15}$$

Let the control time domain be equal to the predicted time domain P, then the optimal performance index function for the control quantity of the electromagnet suspension system is:

$$\begin{aligned} \min J(\boldsymbol{U}_k) &= \left(\boldsymbol{Y}^p{}_{k+1} - \boldsymbol{R}\right)^{\mathrm{T}} \boldsymbol{Q} \left(\boldsymbol{Y}^p{}_{k+1} - \boldsymbol{R}\right) + \boldsymbol{U}_k{}^{\mathrm{T}} \boldsymbol{W} \boldsymbol{U}_k \\ &= \left(\boldsymbol{A}\boldsymbol{Y}_k + \boldsymbol{B}\boldsymbol{U}_k + \boldsymbol{G}\boldsymbol{F} + \delta e_k \boldsymbol{E} - \boldsymbol{R}\right)^{\mathrm{T}} \boldsymbol{Q} \left(\boldsymbol{A}\boldsymbol{Y}_k + \boldsymbol{B}\boldsymbol{U}_k + \boldsymbol{G}\boldsymbol{F} + \delta e_k \boldsymbol{E} - \boldsymbol{R}\right) + \boldsymbol{U}_k{}^{\mathrm{T}} \boldsymbol{W} \boldsymbol{U}_k \end{aligned} \tag{16}$$

Considering the limitation of suspension gap and control current during maglev train operation, the constraints of the indicator function are:

$$\begin{aligned} \boldsymbol{Y}_{\min} < \boldsymbol{Y}^p{}_k < \boldsymbol{Y}_{\max} \\ \boldsymbol{U}_{\min} < \boldsymbol{U}_k < \boldsymbol{U}_{\max} \end{aligned} \tag{17}$$

Where, $\boldsymbol{U}_k = \begin{pmatrix} u(k) & u(k+1) & \cdots & u(k+P-1) \end{pmatrix}^{\mathrm{T}}$ represents control sequence. $\boldsymbol{Q}$ represents the error weight coefficient, which indicates the proximity between the predicted and the expected output. $\boldsymbol{W}$ is the system's weighting coefficient for the control increment. The larger the value of $\boldsymbol{W}$, the smoother the desired change in control, which typically takes a value between 0 and 1.

Let $\boldsymbol{Z} = \boldsymbol{A}\boldsymbol{Y}_k + \boldsymbol{G}\boldsymbol{F} + \delta e_k \boldsymbol{E} - \boldsymbol{R}$, then Equation (16) can be reduced to:

$$\begin{aligned} \min J(\boldsymbol{U}_k) &= \left(\boldsymbol{Z} + \boldsymbol{B}\boldsymbol{U}_k\right)^{\mathrm{T}} \boldsymbol{Q} \left(\boldsymbol{Z} + \boldsymbol{B}\boldsymbol{U}_k\right) + \boldsymbol{U}_k{}^{\mathrm{T}} \boldsymbol{W} \boldsymbol{U}_k \\ &= \frac{1}{2}\left[\boldsymbol{U}_k{}^{\mathrm{T}} \left(2\boldsymbol{B}^{\mathrm{T}}\boldsymbol{Q}\boldsymbol{B} + 2\boldsymbol{W}\right) \boldsymbol{U}_k\right] + 2\boldsymbol{Z}^{\mathrm{T}}\boldsymbol{Q}\boldsymbol{B}\boldsymbol{U}_k + \boldsymbol{Z}^{\mathrm{T}}\boldsymbol{Q}\boldsymbol{Z} \end{aligned} \tag{18}$$

At time t_k, the unknown in Equation (18) is only the vector $\boldsymbol{U}_k$. Therefore, the purpose of rolling optimization is to minimize the objective function J of the control sequence $\boldsymbol{U}_k$. In summary, the predictive control optimization problem of the electromagnet suspension system can be finally reduced to a linear programming problem. Because it is very difficult to solve the nonlinear equation, local numerical optimization is employed to solve a suboptimal solution of the equations.

For the quadratic function J, the variable is $\boldsymbol{U}_k$. Using the Newton iteration method, the control quantity of the suspension system is:

$$\boldsymbol{U}_{\boldsymbol{k}}{}^{j+1} = \boldsymbol{U}_{\boldsymbol{k}}{}^{j} - \left(\boldsymbol{H}^j\right)^{-1} \boldsymbol{J}^j \tag{19}$$

Where $\boldsymbol{J}_j$ is the jacobian matrix of the j_{th} iteration:

$$\boldsymbol{J}_j = \frac{\partial J}{\partial \boldsymbol{U}} = \begin{pmatrix} \frac{\partial J}{\partial u(k)} & \frac{\partial J}{\partial u(k+1)} & \cdots & \frac{\partial J}{\partial u(k+P-1)} \end{pmatrix},$$

$\boldsymbol{H}_j$ is the hessian matrix of the j_{th} iteration:

$$\boldsymbol{H}_j = \frac{\partial^2 J}{\partial \boldsymbol{U}^2} = \begin{pmatrix} \frac{\partial^2 J}{\partial u(k)^2} & \frac{\partial^2 J}{\partial u(k)\partial u(k+1)} & \cdots & \frac{\partial^2 J}{\partial u(k)\partial u(k+P-1)} \\ \frac{\partial^2 J}{\partial u(k+1)\partial u(k)} & \frac{\partial^2 J}{\partial u(k+1)^2} & \cdots & \frac{\partial^2 J}{\partial u(k+1)\partial u(k+P-1)} \\ \vdots & \vdots & \ddots & \vdots \\ \frac{\partial^2 J}{\partial u(k+P-1)\partial u(k)} & \frac{\partial^2 J}{\partial u(k+P-1)\partial u(k+1)} & \cdots & \frac{\partial^2 J}{\partial u(k+P-1)^2} \end{pmatrix}.$$

Assign an initial value $\boldsymbol{U}^0$ to Equation (19), the values of $\boldsymbol{J}^0$, $\boldsymbol{H}^0$, and $\boldsymbol{U}^1$ can be calculated. Repeating the iteration process yields $\boldsymbol{U}^2$, and this iteration continues until a sequence $\boldsymbol{U}^0$, $\boldsymbol{U}^1$, $\boldsymbol{U}^2$, **…** is obtained. This sequence converges to the extreme point of the objective function. If the iteration terminates after the j-th iteration, the control quantity can be taken as $\boldsymbol{U}_k = \boldsymbol{U}^j$.

3.4 Control algorithm

In summary, the operational process of the (MPC) algorithm for the electromagnet suspension system is illustrated in Figure 2:

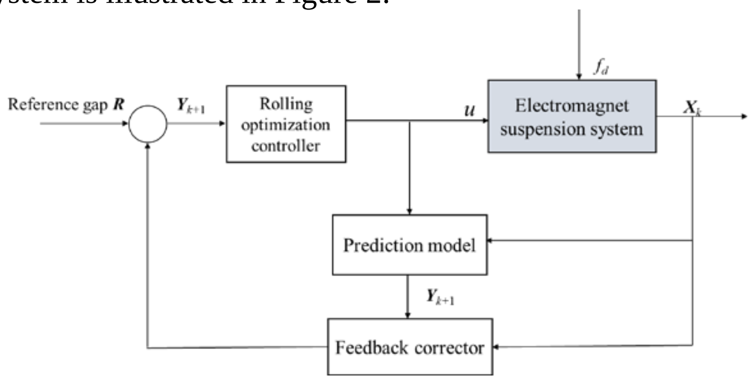

Figure 2: MPC algorithm of single electromagnet suspension system.

(1) Step 1: The state prediction model of the electromagnet is established using its motion equation. At time t_k, the prediction model of the electromagnet suspension system utilizes the current state information to predict system states at future time steps [k +1, …, k + P].

(2) Step 2: Provide feedback correction to the predicted state values of the prediction model output, generating the final predicted output.

(3) Step 3: Minimize the quadratic performance function J to obtain the control sequence $\boldsymbol{U}_k$.

(4) Step 4: The first element $u^*(k)$ from the control sequence $\boldsymbol{U}_k$ is selected as the control quantity of the controlled system, and it is applied to the electromagnet suspension control system.

At the next time step k+1, the new control sequence $\boldsymbol{U}_{k+1}$ is calculated using the same procedure, and the first element $u^*(k+1)$ in the sequence is used as the control quantity of the electromagnet suspension system.

4 Calculation results of numerical model

When constructing the prediction model, ignoring the influence of disturbance force can result in prediction errors, consequently affecting the effectiveness of the controller. In order to determine a more effective MPC algorithm, this study formulates two prediction models—one considering the disturbance force and another disregarding it. Subsequently, the performance of the MPC controller under these two prediction models is calculated.

In order to verify the control performance of the proposed MPC controller in the single-point suspension system, this paper selects the electromagnet suspension gap under PID controller as the reference parameter. A comparative analysis is then conducted to assess the effectiveness of the MPC controller in suppressing the suspension gap fluctuation under different loads. The control logic of the PID controller employed in this study is depicted in Figure 3. Here, K_P, K_I, and K_D denote the proportional, integral, and derivative parameters, with specific values of 7000, 1000, and 800, respectively.

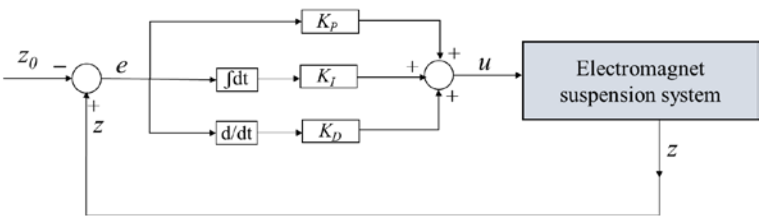

Figure 3: PID control algorithm of single electromagnet suspension system.

In this study, the electromagnet suspension system of the Shanghai TR08 maglev train is taken as the research object. According to the state equation of Equation (9), the dynamic numerical model of the electromagnet suspension system is established using Matlab/Simulink. The main parameters are outlined in Table 1.

Parameter	Value
mass of electromagnet m	330 kg
area of magnetic pole A	0.0259 m^2
number of coils N	290
current of equilibrium point i_0	20 A
gap of equilibrium point z_0	0.01 m

Table 1: Electromagnets information of the TR08 maglev train.

Subsequently, the controller of the electromagnet suspension system is established based on the MPC algorithm proposed in Chapter 3. The pertinent parameters for this MPC algorithm are detailed in Table 2. In this study, the controller's effectiveness is analyzed by comparing the electromagnet fluctuation results in the suspension system under load disturbance. The desired suspension gap for the electromagnet is set at 10 mm. The closer the suspension gap is to this ideal value, the more stable the suspension system, indicating the superior anti-interference effect of the controller.

Parameter	Value
control cycle T	0.001 s
prediction (control) time domain P	20
feedback correction coefficient δ	0.8
state error weight $\boldsymbol{Q}$	$1*\mathrm{I}_{P*P}$

Note: $\mathbf{I}_{P*P}$ is the unit matrix of $P*P$ dimension.

Table 2: Parameter information in the MPC algorithm

Firstly, the suspension operation of electromagnet under the steady load is simulated. From 0 to 5 s, a steady load of 8 kN was gradually applied to the electromagnet, followed the load remains maintained. The calculation results of the electromagnet suspension gap are illustrated in Figure 4. When employing the PID algorithm in the suspension system, the amplitude of the electromagnet fluctuation reaches 2.09 mm. However, under the conventional MPC controller, the amplitude of the electromagnet suspension gap fluctuation is reduced to 1.33 mm, which is 36.4% lower than that of the PID controller. Moreover, under the MPC controller considering the disturbance force in the prediction model (MPC-f_d), the amplitude of the electromagnet suspension gap fluctuation decreased to 0.71 mm, representing a 66.0% reduction compared to the PID controller.

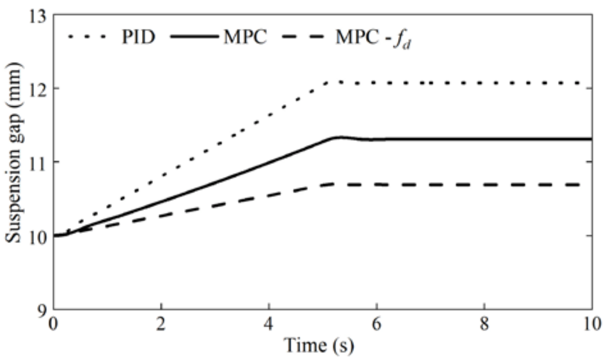

Figure 4: Electromagnet suspension gap under steady load.

Similarly, the suspension test on the electromagnet suspension system subjected to the harmonic load is conducted. The calculation results under different controllers are shown in Figure 5. Employing the PID controller, the amplitude of the suspension gap fluctuation reaches 2.78 mm. When the MPC controller without considering disturbance force is applied, the amplitude of the suspension gap fluctuation of the electromagnet is reduced to 1.80 mm. While under the MPC controller considering the disturbance force in the prediction model (MPC-f_d), the fluctuation amplitude of the suspension gap of the electromagnet is 0.94 mm. Compared with the PID controller, these two MPC controllers reduce the amplitude of the suspension gap fluctuation by 35.3 % and 66.2 %, respectively.

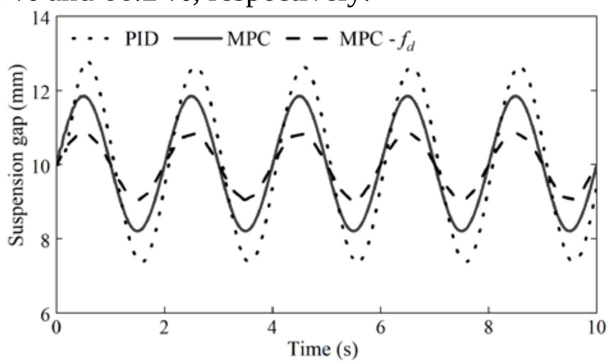

Figure 5: Suspension gap of electromagnet under harmonic load.

Under the disturbance of different loads, the controllers are evaluated for their suspension effectiveness. The most optimal performance among the three controllers is MPC- f_d, followed by MPC, and PID is the least effective. These findings demonstrate that compared with the PID feedback controller, the MPC controller can better suppress the suspension gap fluctuation of the electromagnet and achieve a superior suspension stability effect. This MPC controller offers the advantages of local optimization and feedforward control, which can address the shortcomings associated with global optimization and lag control inherent in traditional control strategies. Moreover, considering the influence of disturbance force when establishing the electromagnet's dynamic response prediction model contributes to achieving more accurate response prediction and obtaining superior control effectiveness.

5 Conclusions and Contributions

In this study, a prediction model for the vertical dynamic response of the electromagnet is constructed according to the disturbed electromagnet motion. Subsequently, the optimization indexes and related constraints for the electromagnet suspension system are established based on the suspension objectives and limitations of the maglev train. Therefore, an MPC controller designed for the suspension electromagnet of the maglev train is proposed. Through numerical calculation, the following conclusions are drawn:

1) In contrast to the PID feedback controller, the MPC controller can predict the future dynamic response of the suspension system and has the benefit of feedforward control. By optimizing the optimal control quantity of the suspension system at each moment in the finite time domain, the MPC controller effectively suppresses the fluctuation of the electromagnet suspension gap under load.

2) When constructing the prediction model for the dynamic response of the electromagnet, accounting for the impact of the disturbance force enhances the control efficacy of the MPC controller.

3) The MPC controller designed based on the disturbed single-point suspension system demonstrates good stability, which can provide a valuable reference for achieving more efficient and stable suspension for high-speed maglev trains.

References

[1] H. W. Lee, K. C. Kim, J. Lee, "Review of maglev train technologies", IEEE Transactions on Magnetics, 42 (7), 1917-1925, 2006.

[2] R. D. Thornton, "Efficient and Affordable Maglev Opportunities in the United States", Proceedings of the IEEE, 97 (11), 1901-1921, 2009.

[3] G. He, "Core Algorithm for Train Control Onboard Equipment", China Railway Science, 39 (3), 110-116, 2018.

[4] J. D. Lindlau, C. R. Knospe, "Feedback linearization of an active magnetic bearing with voltage control", IEEE Transactions on Control Systems Technology, 10 (1), 21-31, 2002.

[5] Y. Khemissi, "Control using sliding mode of the magnetic suspension system", International Journal of Electrical & Computer Sciences, 7373 (30), 1026-1031, 2010.

[6] V. S. S. Starbino, "Design of sliding mode controller for magnetic levitation system", Computers and Electrical Engineering, 78, 184-203, 2019.

[7] C. H. Kim, "Robust Control of Magnetic Levitation Systems Considering Disturbance Force by LSM Propulsion Systems", IEEE Transactions on Magnetics, 53 (11), 1-5, 2017.

[8] J. Zhang, X. Wang, X. Shao, "Design and Real-Time Implementation of Takagi–Sugeno Fuzzy Controller for Magnetic Levitation Ball System", IEEE Access, 8, 38221-38228, 2020.

[9] A. B. Ataşlar, O. Karahan, "Design of a MAGLEV System with PID Based Fuzzy Control Using CS Algorithm", Cybernetics and Information Technologies, 20 (5), 5-19, 2020.

[10] A. Nath, J. Samantaray, S. Chaudhury, B. K. Roy, "Magnetic ball levitation system control using sliding mode control and fuzzy PD+I control: A comparative study", 2015 International Conference on Energy, Power and Environment: Towards Sustainable Growth (ICEPE), Shillong, India, 2015, 1-5.

[11] J. Yang, J. Su, S. Li, X. Yu, "High-Order Mismatched Disturbance Compensation for Motion Control Systems Via a Continuous Dynamic Sliding-Mode Approach", IEEE Transactions on Industrial Informatics, 10 (1), 604-614, 2014.

[12] Y. Gao, Y. Wang, J. Zhang, et al., "A sliding mode periodic adaptive learning operation control method for medium-speed maglev trains", 2020 39th Chinese Control Conference (CCC). Shenyang, China: IEEE, 2020, 548-5553.

[13] F. Ni, S. Mu, J. Kang, J. Xu, "Robust Controller Design for Maglev Suspension Systems Based on Improved Suspension Force Model", IEEE Transactions on Transportation Electrification, 7 (3), 1765-1779, 2021.
[14] A. M. Benomair, A. R. Firdaus and M. O. Tokhi, "Fuzzy sliding control with non-linear observer for magnetic levitation systems," 2016 24th Mediterranean Conference on Control and Automation (MED), Athens, Greece, 2016, 256-261.
[15] M. Abu-Ali, F. Berkel, M. Manderla, S. Reimann, R. Kennel and M. Abdelrahem, "Deep Learning-Based Long-Horizon MPC: Robust, High Performing, and Computationally Efficient Control for PMSM Drives", IEEE Transactions on Power Electronics, 37 (10), 12486-12501, 2022.
[16] Zhao L, Song Y J, Zhang C, et al., "T-GCN: A Temporal Graph Convolutional Network for Traffic Prediction", IEEE Transactions on Intelligent Transportation Systems, 21 (9), 3848-3858, 2020.
[17] P. Gong, Z. Yan Z, W. Zhang, et al., "Trajectory tracking control for autonomous underwater vehicles based on dual closed-loop of MPC with uncertain dynamics", Ocean Engineering, 265, 112697, 2022.
[18] C. Pinto, I. Nieva, S. Mata, et al., "Linear time varying model based model predictive control for lateral path tracking", International Journal of Vehicle Design, 75 (1), 1-22, 2017.
[19] J. Zhang, X. Zhang, X. Y. Zhang, et al, "Trajectory tracking control strategy for oblique driving of 4WIS unmanned vehicle", Transactions of Beijing Institute of Technology, 43 (02), 161-169, 2023.
[20] A. Bemporad, D. Bernardini, R. Long, et al., "Model predictive control of turbocharged gasoline engines for mass production", SAE WCX World Congress Experience. Detroit, Michigan, 2018.
[21] C. W. Son, W. Choi, C. Ahn, "MPC-BASED steering control for backward-driving vehicle using stereo vision", International Journal of Automotive Technology, 18 (5), 933-942, 2017.
[22] A. Jain, L. Chnal, D. S. Brown, et al, "Optimal Cost Design for Model Predictive Control", Proceedings of Machine Learning Research, 144, 1-13, 2021.
[23] R. H. Du, H. F. Hu, K. Gao, et al., "Research on trajectory tracking control of autonomous vehicles based on MPC with variable predictive horizon", Journal of Mechanical Engineering, 58 (24), 275-288, 2022.
[24] H. Chen, J. Chen, H. Lu, et al., "A Modified MPC-Based Optimal Strategy of Power Management for Fuel Cell Hybrid Vehicles", IEEE/ASME Transactions on Mechatronics, 25 (4), 2009-2018, 2020.
[25] Z. C. Liang, H. Zhang, J. Zhao, et al., "Trajectory tracking control of unmanned vehicle based on adaptive MPC", Journal of Northeastern University (Natural Science), 41 (06), 835-840, 2020.
[26] C. F. Xie, K. J. Rao, X. Q. Yang, et al., "Electromagnetic fields and waves", Beijing: Higher Education Press, 2019.